Effect of Thermomigration on Electromigration in SWEAT Structures

Cui, Zhen; Fan, Xuejun; Zhang, Guoqi

DOI
10.1109/EuroSimE56861.2023.10100774

Publication date
2023

Document Version
Final published version

Published in
Proceedings of the 2023 24th International Conference on Thermal, Mechanical and Multi-Physics Simulation and Experiments in Microelectronics and Microsystems (EuroSimE)

2023 24th International Conference on Thermal, Mechanical and Multi-Physics Simulation and Experiments in Microelectronics and Microsystems (EuroSimE) | 979-8-3503-4597-1/23/$31.00 ©2023 IEEE | DOI: 10.1109/EuroSimE56861.2023.10100774

Effect of Thermomigration on Electromigration in SWEAT Structures

Zhen Cui[1], Xuejun Fan[2], Guoqi Zhang[1]

[1]Department of Microelectronics, Delft University of Technology, Delft, 2628 CD, Netherlands
[2]Department of Mechanical Engineering, Lamar University, Beaumont, TX 77710, USA
E-mail: xuejun.fan@lamar.edu

Abstract

This paper investigates thermomigration (TM) and electromigration (EM) in SWEAT structure. Firstly, the distribution of temperature along SWEAT structure during EM is obtained by using finite element (FE) simulation. The FE simulation results show that the temperature is almost uniformly distributed in the most region of narrow line in SWEAT structure, but temperature decreases rapidly at both sides of conductor. Accordingly, the temperature gradient in the narrow line of SWEAT structures is calculated. Then, we apply the obtained temperature and temperature gradient in the governing equation of EM in terms of atomic concentration. The numerical results show that the TM caused by temperature gradient causes the material depletion near both ends of conductor. At the same time, atoms diffuse from the middle region of conductor to both sides driven by the atomic concentration, causing the voids in middle of conductor.

1. Introduction

Electromigration (EM) in interconnects has become a major reliability issue in recent years because of the miniaturization trend to meet the demand of higher performance of microelectronic devices. EM essentially is an enhanced mass transport process driven by high current density [1-8]. The electron wind force, attributed to the momentum exchange between conducting electrons and metal atoms, pushes atoms diffusing from cathode to anode. At the same time, the mass transport driven by temperature gradient, namely thermomigration (TM), is inevitably accompanied with EM [9-11].

In accelerated EM tests, one of the typical structures to explore the effect of temperature and temperature gradient on EM is either the standard wafer-level EM acceleration test (SWEAT) or SWEAT-like structure[6, 10, 12-14]. In this structure, narrow metal line at two ends is connected to large-area pads, allowing atom fluxes between metal line and pads. Using the SWEAT-like structure, it was observed that the void formation occurs at the middle region of metal line, and there is no failure at both ends of metal lines [10, 15, 16]. In recently published papers, Cui *et al*.[10] compared the EM failures in SWEAT structure and Blech structure. It was found that a broad region in the middle of the conductors has void formations. And SWEAT can sustain higher current density and last longer time before EM damage, compared to Blech structure. This type of damage was believed to be caused by TM at elevated current density.

Kim et al.[17] obtained the analytical expressions for estimating the temperature profile along SWEAT-like structure due to the Joule heating generated by a high current density. It was found that the SWEAT structure with 12 μm narrow line has the maximum temperature in the center of conductor, and the temperature gradually decreases from the center to both ends of conductor. Jing *et al.* [18] did the electrical-thermal FEM simulation to obtain the temperature distribution in SWEAT structure with 10 um narrow line. A current density of 15 MA/cm^2 was used in simulation. Although simulation results showed that there exists a significant temperature gradient along conductor length, the impact of TM on EM was ignored in analyzing failure results. In recent papers, Cui *et al*.[10] obtained several important conclusions about the impact of TM on EM with increasing current density. Based on the results, to be shown in this paper, most of the Joule heating generated in the metal lines is dissipated through the silicon substrate. Only a very small fraction of heat was conducted through metal lines. To obtain the analytical solution, an over-simplified temperature distribution was obtained with the introduction of "modified thermal conductivity" in [10]. To further evaluate the effect of temperature and temperature gradient, a more accurate approach in obtaining temperature and temperature gradient is required.

In this paper, the coupled electrical and temperature modeling in SWEAT structures during EM testing are performed using finite element simulation. Temperature variations under different current densities due to Joule heating effect are obtained. After that, we apply the obtained temperature and temperature gradient to the 1D governing equation of EM with TM, to evaluate the impact of actual temperature profiles.

2. Governing Equation

The coupled thermal-electrical governing equations can be expressed as follows,

$$\nabla \cdot \left(\frac{\nabla V}{\rho}\right) = 0 \tag{1}$$

$$\nabla \cdot (k\nabla T) + \frac{1}{\rho}|\nabla V|^2 = 0 \tag{2}$$

where T is temperature, V is the electrical potential, k is thermal conductivity, and ρ is the electric resistivity. The joule heating is expressed by the second term on the left side in Equation (2). Above equations can be solved with the appropriate boundary conditions. Steady-state

979-8-3503-4597-1/23/$31.00 ©2023 IEEE

temperature distribution is assumed. The relationship between current density $\boldsymbol{j}$ and the electrical potential V is as follows:

$$\boldsymbol{j} = -\frac{\nabla V}{\rho} \tag{3}$$

After the electrical and temperature fields are solved, the governing equation in terms of atomic concentration in a 1D stress-free metal line during EM can be obtained by using following equation (4). Please see details in refer. [10] for the derivation of Eq. (4).

$$\frac{1-f}{C_a}\frac{\partial C_a}{\partial t} = D_a\left[-\frac{Z^* e\rho j}{k_B T_{\mathrm{m}}}\frac{\partial C_a}{\partial x} + \frac{\partial^2 C_a}{\partial x^2} + \frac{Q^*}{k_B {T_{\mathrm{m}}}^2}\frac{\partial C_a}{\partial x}\frac{dT}{dx} + \frac{Q^* C_a}{k_B {T_{\mathrm{m}}}^2}\frac{d^2 T}{dx^2}\right] \tag{4}$$

where C_a is the atomic concentration, D_a is the atomic diffusivity, Z^* is the effective charge number ($Z^*>0$), e is the elementary charge, k_B is the Boltzmann constant, and Q^* is the heat of transport.

3. Finite Element Model

FE simulation was performed by using ANSYS 19.1 software to obtain the distribution of temperature in the SWEAT structure. The FE model was constructed based on the SWEAT structure used in experiments in refer. [6, 10]. As shown in Fig. 1, a 1 µm-thick SiO_2 layer was created on a 200 µm-thick Si substrate. The width and length for SiO_2 layer are 200 µm and 1100 µm, respectively. Then, a 300 nm-thick TiN layer was built on SiO_2 layer. After that, a 200 nm-thick Al layer was constructed as SWEAT structure. The length and width of narrow line in SWEAT are 800 µm and 5 µm width, respectively. In an actual EM test set-up, the silicon substrate is 1000 mm by 1000 mm. We took a small portion of the silicon substrate in our FE model as temperature is almost uniform beyond certain distance from the metal line.

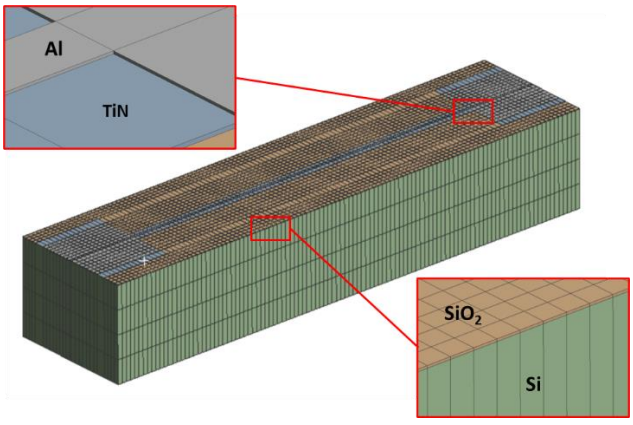

Fig. 1. Global model for SWEAT structure, and local regions for Al conductor, TiN layer, SiO_2 layer, and Si substrate.

The global thermal-electric coupled field model used the regular hexahedral Solid-186 element in ANSYS, where 7860 solid elements for SWEAT structure was used. According to the testing conditions for EM in refer. [6, 10], following boundary conditions are applied:

(1) On one end of the Al layer, the voltage potential is set grounded (zero), while the other end is given voltages of 1440 mV, 864 mV, and 288 mV, to generate 1, 3, and 5 MA/cm^2 current density in the conductor.

(2) The temperature at bottom of Si substrate was set as 525 K (~ 250 °C).

(3) The thermal isolation was assumed for the other surface of structures (radiation effect neglected).

The thermal and electrical parameters used in FE simulation are listed in Table 1.

Table 1. Material properties of Al used in simulations.

Property	Value
Al electrical resistivity	3.22×10^{-8} Ohm·m
Al thermal conductivity	239 W/(m·ºC)
TiN electrical resistivity	6×10^{-6} Ohm·m
TiN thermal conductivity	5 W/(m·ºC)
SiO_2 thermal conductivity	0.15 W/(m·ºC)
Si thermal conductivity	50 W/(m·ºC)

4. Temperature and Temperature Gradient

Fig.2 (a) and (b) show the contours of current density and temperature in SWEAT structure under current density of 5 MA/cm^2. From Fig. 2 (a), the current density in narrow line is uniformly distributed over the entire region except both ends. From Fig. 2(b), the middle segment of narrow line has the maximum temperature of 582 K, and the temperature decreases rapidly at the region near both ends. The temperature at pads is 525 K that is the same with the ambient temperature.

Fig. 3 plots the temperature along the length of SWEAT structure under current densities of 1 MA/cm^2, 3 MA/cm^2 and 5 MA/cm^2. The locations from 0 to 150 µm and 950 to 1100 µm represent the region for big pads. The location from 150 µm to 950 µm represents the narrow line. It can be seen that the SWEAT structure has maximum temperature at the middle region, and the temperature is almost uniformly distributed at the region from 200 µm to 900 µm. This is different from the analytical solution for temperature profile presented in [10]. Moreover, the maximum temperature increases from 527 K to 582 K with the increasing current density from 1 MA/cm^2 to 5 MA/cm^2, which are consistent with the results of analytical solutions in [10]. At both sides of narrow line, temperature drops rapidly. At big pads, the temperature decreases to ambient temperature of 525 K.

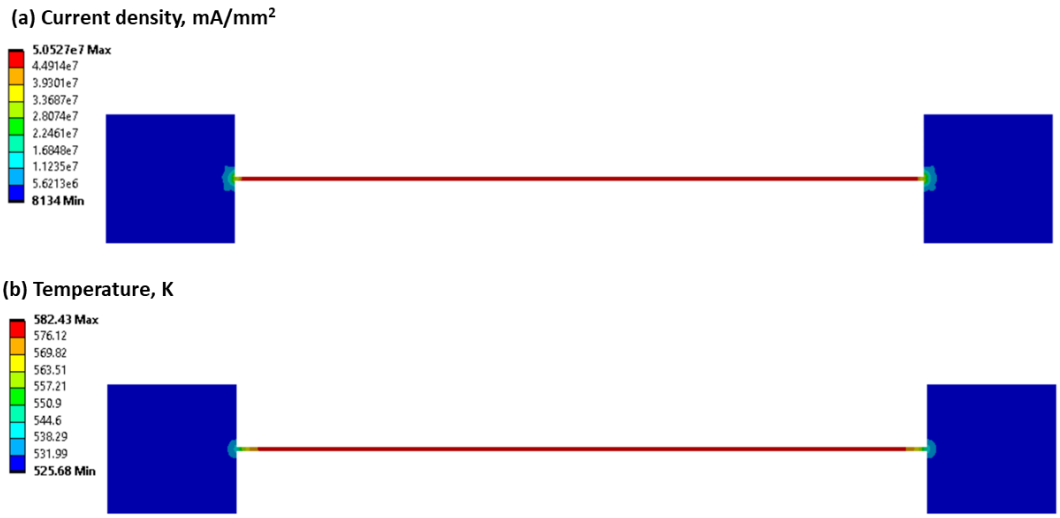

Fig. 2 (a) Current density contour and (b) temperature conductor in SWEAT structure under current density of 5 MA/cm^2.

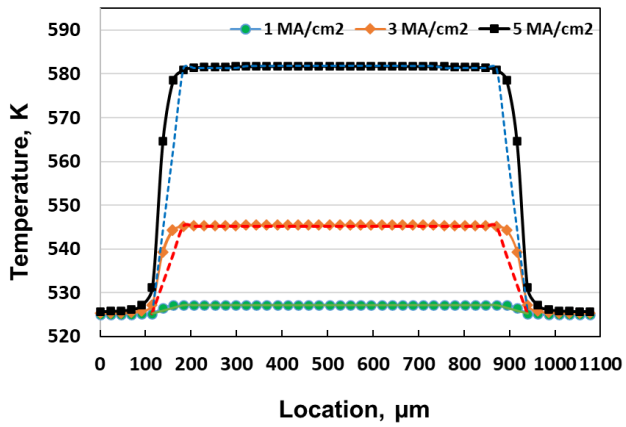

Fig. 3. Temperature distribution along the length of SWEAT structure under current density of 1/3/5 MA/cm^2.

5. Atomic Concentration C_a

To calculate C_a, we only considered the narrow line in SWEAT structure from 150 μm to 950 μm (in a 800 μm conductor). To solve Eq. (4):

(1) Boundary condition: C_a at both ends of narrow line was set as a constant value (C_a(150 μm, t) = C_a(950 μm, t) = C_{a0}).

(2) Initial condition: C_a(x, 0)=C_{a0} for entire length of conductor.

(3) The temperature along the conductor length was simplified as a piecewise function as the dash line plotted in Fig. 3. The temperature linearly increases from both sides to middle region and keep constant temperature from 200 μm to 900 μm. The magnitude of temperature gradient in narrow line under current densities of 1/3/5 MA/cm^2 are listed in Table 2.

(4) According to the FEM results, a constant current density along conductor was considered in calculation.

Moreover, following parameters are used for solving Eq. (4) [10, 19, 20]: atomic volume (Ω) is 1.66×10-29 m^3, electrical resistivity (ρ) is 3.22×10-8 Ohm·m, electrical charge (e) is 1.6×10-19 C, Effectivity charge number (Z^*) is 1.1, heat of transport (Q^*) is 0.3, vacancy volume relaxation factor (f) is 0.7, and atomic diffusivity (D_a) is $8\times10^{-8}\exp(-0.57\text{eV}/k_B\text{T})$ m/s.

Table 2. Input of temperature gradient along SWEAT structure in calculations for atomic concentration. Location from 150 μm to 950 μm is the region for narrow Al line of SWEAT structure.

Current density	Temperature gradient in different region		
	150-200 μm	200-900 μm	900-950 μm
1 MA/cm^2	230 K/cm	0	-230 K/cm
3 MA/cm^2	2280 K/cm	0	-2280 K/cm
5 MA/cm^2	6430 K/cm	0	-6430 K/cm

Fig. 4 plots the results for the C_a/C_{a0} at 5/10/15 h along the SWEAT structure under current density of 3 MA/cm^2. The atomic concentration starts to decrease at the region near both sides, due to the temperature gradient at both sides causes atoms diffusing out of conductor. Moreover, the region with C_a decreasing spreads from both sides to middle region with time increasing. And there is no temperature gradient in the middle region. Therefore, the decrease of atomic concentration is due to the atomic concentration near both sides is lower than that in middle region, the atomic concentration gradient drives atoms at the middle region diffusing to both sides.

Fig. 5 plots the variations of C_a/C_{a0} at 5 h under different current densities. Under 1 MA/cm^2 current density, C_a/C_{a0} changes slightly. With the increasing current density, the conductor near both sides has lower atomic concentration. And the region with C_a decreasing under 5 MA/cm^2 is larger than those under 1 and 3 MA/cm^2. Those results indicate that the conductor would form void at the region near both sides. And, the region with void formation could spread to the middle region of conductor.

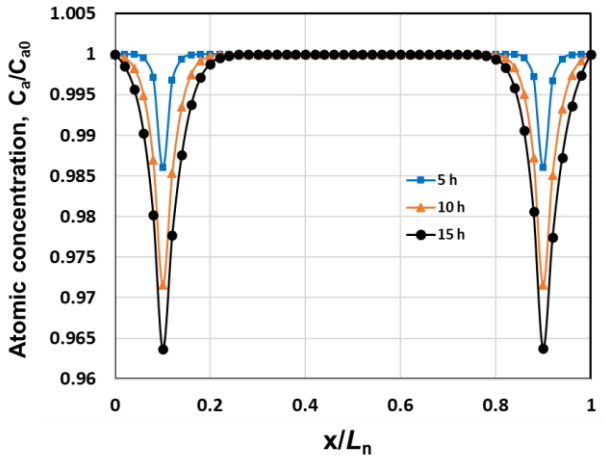

Fig. 4. C_a/C_{a0} along the length of SWEAT structure at 5h, 10 h, and 15h under current density of 3 MA/cm2. L_n is equal to 800 μm that is the length of narrow Al line.

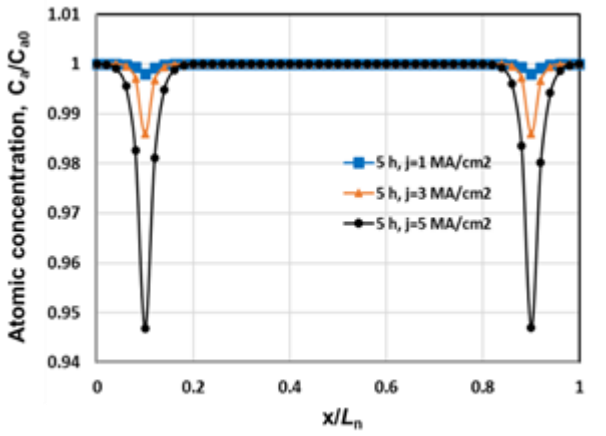

Fig. 5. C_a/C_{a0} along the length of SWEAT structure at 5 h under current densities of 1, 3, and 5 MA/cm^2.

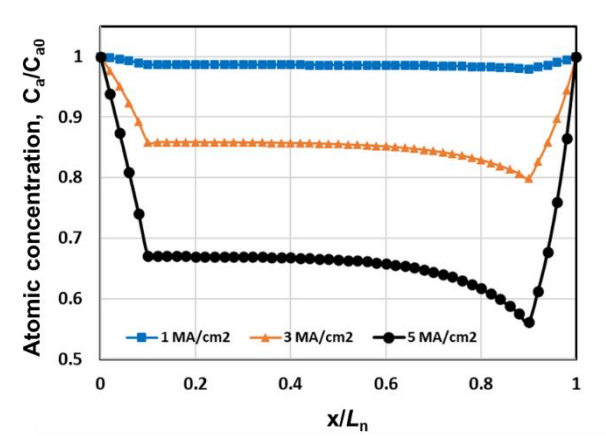

Fig. 6. C_a/C_{a0} along the length of SWEAT structure at steady state under current densities of 1, 3, and 5 MA/cm^2.

At steady state, C_a/C_{a0} at the entire conductor decreases, as shown in Fig. 6. Under the current density of 1 MA/cm2, C_a/C_{a0} reaches the steady state at time around 2.5×10^5 s, and C_a/C_{a0} slightly changes, indicating no void formation for SWEAT structure under j=1 MA/cm^2. When the current density increases to 3 MA/cm^2 and 5 MA/cm^2, C_a/C_{a0} reaches the steady state at time around 1.5×10^5 s and 1×10^5 s, respectively. And C_a/C_{a0} decreases sharply at the region near both sides, due to the temperature gradient. At the middle region, C_a/C_{a0} decreases slowly and reaches the minimum value near the anode side.

4. Conclusions

Electrical-thermal simulation results showed that the SWEAT structure has the uniform temperature at the middle region of narrow line. At the region near both ends of narrow line, the temperature decreases rapidly, causing high temperature gradients. By using the results of temperature field from FE simulation, the numerical results showed that under the current density of 1MA/cm^2, the impact of TM on EM is negligible. However, when the current density increases to 3 MA/cm^2, TM leads to an obvious decrease of atomic concentration near both sides of conductor. Subsequently, atoms at the middle region would slowly diffuse to both sides under the driving force of atomic concentration gradient, causing the decrease of atomic concentration for entire SWEAT structure.

References

1. Cui, Z., Fan, X., Zhang, G., 2019. General coupling model for electromigration and one-dimensional numerical solutions. Journal of Applied Physics 125, 105101.
2. Cui, Z., Fan, X., Zhang, G., 2021. Molecular dynamic study for concentration-dependent volume relaxation of vacancy. Microelectronics Reliability 120, 114127.
3. Dandu, P. and X. Fan. *Assessment of current density singularity in electromigration of solder bumps*. in *2011 IEEE 61st Electronic Components and Technology Conference (ECTC)*. 2011. IEEE.
4. Dandu, P., et al., *Finite element modeling on electromigration of solder joints in wafer level packages.* Microelectronics Reliability, 2010. **50**(4): p. 547-555.
5. Dandu, P., X. Fan, and Y. Liu. *Some remarks on finite element modeling of electromigration in solder joints*. in *2010 Proceedings 60th Electronic Components and Technology Conference (ECTC)*. 2010. IEEE.
6. Cui, Z., et al., *Coupling model of electromigration and experimental verification–Part I: Effect of atomic concentration gradient.* Journal of the Mechanics and Physics of Solids. Volume 174, p. 105257, 2023.
7. Taner, O., K. Kijkanjanapaiboon, and X. Fan. *Does current crowding induce vacancy concentration singularity in electromigration?* in *2014 IEEE 64th Electronic Components and Technology Conference (ECTC)*. 2014. IEEE.
8. Cui, Z., *Multi-Physics Driven Electromigration Study: Multi-Scale Modeling and Experiment*, Doctor Dissertation, 2021, Delft University of Technology.
9. Cui, Z., Zhang, Y., Hu, D., Vollebregt, S., Fan, J., Fan, X., Zhang, G., 2022b. Effects of temperature and grain size on diffusivity of aluminium: electromigration experiment and molecular dynamic

simulation. Journal of Physics: Condensed Matter 34, 175401
10. Cui, Z., et al., *Coupling model of electromigration and experimental verification–Part II: Impact of thermomigration.* Journal of the Mechanics and Physics of Solids. Volume 174, p. 105256, 2023.
11. Ye, H., C. Basaran, and D.J.A.P.L. Hopkins, *Thermomigration in Pb–Sn solder joints under joule heating during electric current stressing.* 2003. **82**(7): p. 1045-1047.
12. Lee, T.C., et al. *Comparison of isothermal, constant current and SWEAT wafer level EM testing methods*. in *2001 IEEE International Reliability Physics Symposium Proceedings. 39th Annual (Cat. No. 00CH37167)*. 2001. IEEE.
13. Blech, I. and K.J.A.P.L. Tai, *Measurement of stress gradients generated by electromigration.* 1977. **30**(8): p. 387-389.
14. Blech, I. and C.J.A.P.L. Herring, *Stress generation by electromigration.* 1976. **29**(3): p. 131-133.
15. Giroux, F., et al. *Wafer-level electromigration tests on NIST and SWEAT structures*. in *Proceedings International Conference on Microelectronic Test Structures*. 1995. IEEE.
16. Giroux, F., et al. *Current and temperature distribution impact on electromigration failure location in SWEAT structure*. in *Proceedings of 1994 IEEE International Conference on Microelectronic Test Structures*. 1994. IEEE.
17. Jonggook, K., V. Tyree, and C. Crowell. *Temperature gradient effects in electromigration using an extended transition probability model and temperature gradient free tests. I. Transition probability model*. in *1999 IEEE International Integrated Reliability Workshop Final Report (Cat. No. 99TH8460)*. 1999. IEEE.
18. Jing, J., L. Liang, and G. Meng, *Electromigration simulation for metal lines.* J. Electron. Packag., 2010. **132 (1)**
19. Cui, Z., X. Fan, and G. Zhang. *Implementation of Fully Coupled Electromigration Theory in COMSOL*. in *2022 IEEE 72nd Electronic Components and Technology Conference (ECTC)*. 2022. IEEE.
20. Cui, Z., X. Fan, and G. Zhang, *Implementation of General Coupling Model of Electromigration in ANSYS*, in *2020 IEEE 70th Electronic Components and Technology Conference (ECTC)*. 2020. p. 1632-1637.